

Systems Biotechnology

Biotechnology and Bioengineering
DOI 10.1002/bit.22932

Modeling of uncertainties in biochemical reactions

Ljubiša Mišković, Vassily Hatzimanikatis

Laboratory of Computational Systems Biotechnology,
Ecole Polytechnique Fédérale de Lausanne (EPFL), CH--1015 Lausanne,
Switzerland.

Correspondence to:

Vassily Hatzimanikatis

EPFL / SB / ISIC / LCSB

CH H4 625 (Bat. CH)

Station 6

CH-1015 Lausanne, Switzerland

Tel: +41 21 693 98 70; Fax: +41 21 693 98 75;

Email: vassily.hatzimanikatis@epfl.ch

© 2010 Wiley Periodicals, Inc.

Received July 13, 2010; Revised August 10, 2010; Accepted August 17, 2010

Abstract

Mathematical modeling is an indispensable tool for research and development in biotechnology and bioengineering. The formulation of kinetic models of biochemical networks depends on knowledge of the kinetic properties of the enzymes of the individual reactions. However, kinetic data acquired from experimental observations bring along uncertainties due to various experimental conditions and measurement methods. In this contribution, we propose a novel way to model the uncertainty in the enzyme kinetics and to predict quantitatively the responses of metabolic reactions to the changes in enzyme activities under uncertainty. The proposed methodology accounts explicitly for mechanistic properties of enzymes and physico-chemical and thermodynamic constraints, and is based on formalism from systems theory and metabolic control analysis. We achieve this by observing that kinetic responses of metabolic reactions depend: (i) on the distribution of the enzymes among their free form and all reactive states; (ii) on the equilibrium displacements of the overall reaction and that of the individual enzymatic steps; and (iii) on the net fluxes through the enzyme. Relying on this observation, we develop a novel, efficient Monte Carlo sampling procedure to generate all states within a metabolic reaction that satisfy imposed constraints. Thus we derive the statistics of the expected responses of the metabolic reactions to changes in enzyme levels and activities, in the levels of metabolites, and in the values of the kinetic parameters. We present aspects of the proposed framework through an example of the fundamental three-step reversible enzymatic reaction mechanism. We demonstrate that the equilibrium displacements of the individual enzymatic steps have an important influence on kinetic responses of the enzyme. Furthermore, we derive the conditions that must be satisfied by a reversible three-step enzymatic reaction operating far away from the equilibrium in order to respond to changes in metabolite levels according to the irreversible Michaelis-Menten kinetics. The efficient sampling procedure allows easy, scalable,

implementation of this methodology to modeling of large-scale biochemical networks.

● **Introduction**

Advancements in genome sequencing have sparked an intensive development of fields that rely on 'omics' data. However, the development in the area of kinetic modeling of large metabolic networks does not follow the same pace. Although metabolomic and fluxomic data are widely available, large-scale kinetic models are very scarce in the literature (Goodacre et al., 2004; Breitling et al., 2008; Jamshidi and Palsson, 2008). The efforts in this line of research have been hindered by the lack of pertinent information of the kinetic properties of enzymes in a metabolic network. Experimentally measured kinetic properties of enzymes come necessarily with an extend of uncertainty that originates from differences in experimental conditions and measurement techniques (Wang et al., 2004). In addition, it has been argued that parameter values estimated from the experimental data and directly used into a model are likely to lead to thermodynamical inconsistencies (Liebermeister and Klipp, 2006). Another stumbling block stems from the difficulty to establish rate laws and parameter values for each reaction in large-scale metabolic networks that might contain several hundreds or even thousands of reactions (Jamshidi and Palsson, 2010).

In an attempt to characterize the kinetic responses of metabolic networks in the presence of uncertainty a number of methods that explore the parameter space emerged in the literature (Thomas and Fell, 1994; Petkov and Maranas, 1997; Alves and Savageau, 2000; Almaas et al., 2004). More recently, within the context of Metabolic Control Analysis (MCA), Hatzimanikatis and co-workers have proposed a Monte Carlo sampling procedure for the generation of populations of kinetic models that allow the identification of the rate-limiting steps in metabolic networks (Wang et al., 2004; Wang and Hatzimanikatis, 2006b,a). Motivated by

ideas in this work, Liao and co-workers used a Monte Carlo algorithm to sample the parameter space in order to obtain a set of models that all reach the same prescribed steady state (Tran et al., 2008; Rizk and Liao, 2009; Contador et al., 2009). However, this method is computationally intensive and it can be prohibitive for the analysis of large-scale metabolic networks.

Although all aforementioned methods that employ parameter space search circumvent the problem of acquiring kinetic data, there are challenges still to be addressed. The kinetic parameters in each of the reactions are related through the equilibrium constants that are dependent on the standard free energy change of the reaction (Cornish-Bowden and Cardenas, 2000; Nelson and Cox, 2005; Beard and Qian, 2008; Ross, 2008). These dependencies imply that the kinetic parameters' space is constrained in a very intricate way, which might reduce the sampling efficiency especially in the case of modeling of large-scale metabolic networks. On the other hand, ignoring possible constraints might result in a population of computed models containing a subset of thermodynamically and physico-chemically inconsistent models (Steuer et al., 2006; Grimbs et al., 2007).

In their approach, Hatzimanikatis and co-workers randomly sampled the degree of saturation of the active site of an enzyme and used it subsequently to compute the sensitivities of reaction responses to the variations of metabolite concentrations and parameters, known within MCA as "elasticities" (Wang et al., 2004; Wang and Hatzimanikatis, 2006b,a). These works laid a foundation for a computational framework for the Optimization and Risk Analysis of Complex Living Entities (ORACLE) that integrates biological information from different sources into a mathematical formalism enabling to identify the rate-limiting steps in biochemical pathways (Mišković and Hatzimanikatis, 2010). In this contribution, we focus on deriving the elasticities as a function of a fractional distribution of the enzyme among its states, the free enzyme and its intermediary complexes, and the displacement from the thermodynamic equilibrium of the individual enzymatic

steps. We then exploit the assumption that the total amount of enzyme is preserved in the course of reaction, and we sample randomly the space of enzyme states. Consequently, we use so obtained population of enzyme states, along with the equilibrium displacements of the individual elementary enzymatic steps of the reaction, to compute the elasticities. In our computation, we consider explicitly that the individual equilibrium displacements are constrained by the equilibrium displacement of the overall reaction which, in turn, depends on the thermodynamically feasible metabolite concentrations in the network. So, the proposed computational method explicitly integrates the conservation of the total amount of the enzymes, and the information about reactions thermodynamics and concentration of metabolites.

In contrast to widely used in the literature Markov Chain Monte Carlo methods, the method we propose here does not suffer from the slow mixing property (Schellenberger and Palsson, 2009). This sampling mechanism exploits the specific structure of the underlying constraints and is efficient in the sense that it generates samples of kinetic data that satisfy the imposed constraints and any prescribed distribution of enzyme states at each iteration. The scalability of the sampling mechanism provides means to build genome-scale kinetic models.

Results and Discussion

Fundamental enzyme mechanism

We study here the reversible Michaelis-Menten enzymatic mechanism as shown in Fig. 1. The reversible Michaelis-Menten kinetics is a three-step mechanism containing three separate steps: (i) binding the enzyme E to the substrate S , (ii) the reversible catalytic conversion between the enzyme-substrate ES and the enzyme-product EP complexes, and (iii) binding of the enzyme E to product P (Heinrich and Schuster, 1996). The concentration of the total enzyme E_T , the first-order rate constants k_{1b} , k_{2f} , k_{2b} and k_{3f} , and the second-order rate constants k_{1f} and k_{3b} ,

along with the concentrations of the substrate S and the product P , constitute the vector of parameters for this mechanism as follows

$$p = [E_T, k_{1f}, k_{1b}, k_{2f}, k_{2b}, k_{3f}, k_{3b}, S, P]^T. \quad (1)$$

The operator $(\cdot)^T$ denotes the transpose. In general, p contains three groups of parameters: (i) p_i - conserved concentrations of total enzymes; for single-enzyme reactions it consists of E_T , while in the case of substrate channeling it includes the total levels of all involved enzymes; (ii) p_r - rate constants of the elementary reaction steps; and (iii) p_n - other parameters, such as S and P for the reversible Michealis-Menten mechanism. Therefore, in the more general case the parameter vector, p , can be written as:

$$p^T = [p_i^T, p_r^T, p_n^T]. \quad (2)$$

It is assumed that the amount of the total enzyme is conserved in the course of reaction

$$E_T = E + ES + EP. \quad (3)$$

For a fixed amount of total enzyme, E_T , only two of three enzyme states, E , ES and EP , can be considered as independent. Assuming that the complexes ES and EP are the independent variables, we derive analytical expressions according to the Metabolic Control Analysis formalism for the reduced stoichiometric matrix M_R , the steady-state flux matrix U , the elasticity matrices Ξ and Π which represent the normalized sensitivities of the individual enzymatic forward and backward reaction rates, u_{if} and $u_{ib}, i = 1, 2, 3$ with respect to the concentrations of the intermediate complexes, ES and EP , and the parameters, p , respectively (see Table 1 for definitions and Table 2 for matrix expressions). Subsequently, we assume that the net rate of the reaction is *positive*, i.e. the reaction operates in the direction from the substrate S to the product P , which in turn implies that $\gamma_i \leq 1, \forall i = 1, 2, 3$.

From a systems theory perspective, if we consider the single enzyme as the system, and the substrates and products as external inputs (parameters), the derived MCA elements correspond to the concentration and the flux control coefficients with respect to the parameters (including S and P), i.e., to the normalized sensitivities of the net reaction rate, $u_{net} = u_{if} - u_{ib}$, with respect to the parameters (cf Table 2 and Eqs. 11 and 12 in Methods). However, if we consider the enzymes as components of a metabolic network, with S and P as two of its dependent metabolites, i.e. variables, these control coefficients are in fact the enzyme elasticities with respect to the substrate concentration S , the product concentration P and the enzyme activity. In what follows, we will refer to these quantities as metabolite and flux elasticities in order to denote their role within metabolic networks. The MCA elements given in Table 2 can also be used to compute the control coefficients with respect to the rate constants (Kholodenko et al., 1994).

Generating populations of elasticities

By inspecting Table 2, it is observed that if we know the ratios $.8mm E / -.8mm E_T$, $.8mm ES / -.8mm E_T$ and $.8mm EP / -.8mm E_T$, we can compute Ξ and Π . In general, these ratios are not known. Even when some experimentally observed data are available, the uncertainty introduced due to different experimental conditions makes impossible a precise quantification of these ratios. To generate these quantities, while taking into account the above mentioned uncertainties, we employ the Monte Carlo sampling technique as follows.

Equation 3 divided by E_T defines a simplex in the three-dimensional space of enzyme species as illustrated in Fig. 2. If we assume that the enzyme appears with the equal probability in its three states E , ES and EP , we can sample uniformly and efficiently the enzyme species over this surface, and thus we can explore the complete three-dimensional subspace of enzyme states that satisfies the constraint in Eq. 3. In the case where the experimental data indicate that the enzyme stays

predominantly in one or two of its species, or that any of the enzyme states follow an observed or hypothesized distribution, we construct a non-uniform distribution over the simplex from which the triplets of the enzyme species are sampled. The resulting random triplets of the ratios $.8mm E / -.8mm E_T$, $.8mm ES / -.8mm E_T$ and $.8mm EP / -.8mm E_T$ can then be used to compute the populations of the matrices Ξ and Π . The relationships between the enzyme states and the elasticities with respect to the unidirectional rate constants can also be derived as it was done previously in (Kholodenko et al., 1994)

The metabolite and the flux elasticities depend on the equilibrium coefficients γ_i and the steady-state net flux U_{net} , in addition to the ratios of the enzyme states (see Eqs. 11 and 12 in Methods). The values of the net steady-state flux U_{net} can be estimated using methods from the Flux Balance Analysis (FBA) and Metabolic Flux Analysis (MFA) (Varma and Palsson, 1993b,a; Teusink et al., 2000). On the other hand, the equilibrium displacement Γ , that can easily be extracted from the experimental data, constrains the equilibrium coefficients γ_i (see Methods). This allows to estimate γ_i 's using the knowledge of Γ and the available genomic and kinetic information.

Overall, we show that provided that the equilibrium coefficients and the net steady-state flux are known, the randomly generated samples of the enzyme species triplets allow for computing the populations of flux and metabolite elasticities that correspond to the thermodynamically and physio-chemically feasible states of a reaction. The statistical characteristics of the resulting elasticities can further be analyzed using various data-mining methods.

Irreversible Michaelis-Menten kinetic mechanism

The irreversible Michaelis-Menten kinetics has been used in almost every mathematical model of metabolic networks. In this section, we identify the

conditions under which the general three-step kinetic mechanism presented in the previous section reduces to the irreversible Michaelis-Menten kinetics.

The irreversible Michaelis-Menten kinetic mechanism characterizes a reaction that kinetically does not favor the binding of the free enzyme to the product. Therefore, for this mechanism the enzyme elasticities with respect to the substrate are uniformly distributed between 0 and 1. In addition, the elasticities with respect to the product are near zero. We investigate under which conditions it is possible to simulate this behavior by using the reaction structure shown in Fig. 1.

In the literature, the common assumption that leads to the use of the irreversible Michaelis-Menten kinetics is that it well describes the kinetic mechanism of the uni-uni reactions away from the equilibrium, i.e. having the equilibrium displacement $\Gamma \ll 1$. However, we find that for a reaction to follow this kinetic mechanism there are additional conditions to be satisfied. In a reaction including three enzymatic reaction steps (Fig. 1), the overall equilibrium displacement is related to the equilibrium coefficients of the individual reaction steps according to the following equation:

$$\Gamma = \gamma_1 \gamma_2 \gamma_3 \quad (4)$$

which implies that the equilibrium coefficients are bounded as follows: $\Gamma \leq \gamma_i \leq 1$ (Fig. 3). We first assume that: (i) the enzyme operates away from the equilibrium, that is $\Gamma = 0.01$, with the equilibrium coefficient for the first enzymatic step being $\gamma_1 \approx \Gamma$, and $\gamma_2 = \gamma_3 \approx 1$; and (ii) the formation of the enzyme-product complex EP is not favorable, i.e. EP appears with a low probability during the course of the reaction.

Based on these two assumptions we generated 2000 random sets of the enzyme states and we analyzed the distributions of the computed populations of elasticities (Fig. 4, panel A). Although this reaction is away from the equilibrium, the resulting elasticities do not correspond to the irreversible Michaelis-Menten kinetics. The influence of the product concentration is not negligible, and the

population of the corresponding flux elasticities is distributed between -1 and 0.

We can better understand the origins of this behavior by deriving the analytical expressions for the flux elasticities:

$$\varepsilon_S^{u_{net}} = \frac{\frac{E}{E_T} + \gamma_2 \gamma_3 \frac{ES}{E_T} + \gamma_3 \frac{EP}{E_T}}{1 - \gamma_1 \gamma_2 \gamma_3} \quad (5)$$

$$\varepsilon_P^{u_{net}} = -\frac{\gamma_1 \gamma_2 \gamma_3 \frac{E}{E_T} + \gamma_2 \gamma_3 \frac{ES}{E_T} + \gamma_3 \frac{EP}{E_T}}{1 - \gamma_1 \gamma_2 \gamma_3}. \quad (6)$$

Considering that E/E_T , ES/E_T and EP/E_T are smaller than 1, for reactions away from the equilibrium ($\gamma_1 \gamma_2 \gamma_3 \ll 1$) the denominators in Eqs. 5 and 6 are approximatively equal to 1, and the first term in the numerator of Eq. 6 can be neglected since $\gamma_1 \gamma_2 \gamma_3 E/E_T \ll 1$. Hence, these two expressions reduce to

$$\varepsilon_S^{u_{net}} \approx \frac{E}{E_T} + \gamma_2 \gamma_3 \frac{ES}{E_T} + \gamma_3 \frac{EP}{E_T} \quad (7)$$

$$\varepsilon_P^{u_{net}} \approx -\gamma_2 \gamma_3 \frac{ES}{E_T} - \gamma_3 \frac{EP}{E_T}. \quad (8)$$

These equations lead to two important observations: (i) the elasticities of the enzymes are explicit functions of the distribution of the enzymes among their different states and the individual equilibrium displacements; (ii) for enzymes that operate far from their equilibrium, when the displacement from the equilibrium is primarily contained in the first step ($\gamma_1 \approx \Gamma$), taking into consideration the conservation of the total enzyme it follows that $\varepsilon_S^{u_{net}} \approx 1$ and $\varepsilon_P^{u_{net}} \approx -\frac{ES}{E_T} - \frac{EP}{E_T}$, which in turn implies that $\varepsilon_P^{u_{net}}$ is distributed between -1 and 0. These observations suggest that large displacement from equilibrium and even high negative Gibbs free energy are not sufficient conditions to describe the reactions following the irreversible Michaelis-Menten kinetics.

From the above analytical expressions for the flux elasticities, one can

distinguish several possible scenarios for the validity of irreversible Michaelis-Menten mechanism:

- *The last elementary step is far away from the equilibrium, $\gamma_3 \ll 1$, whereas the equilibrium coefficients of the first, γ_1 , and of the intermediary step, γ_2 , are close to 1 (due to the constraint given in Eq. 4). In addition, the intermediate complex EP appears with a low probability, which in turn results in the equal probability for the enzyme species E and ES to form and dissolve. The Gibbs free energy reaction coordinate profiles corresponding to this case are given in Fig. 5. Since the concentration of EP is negligible with respect to the concentrations of E and ES , and considering that $\gamma_3 \ll 1$, we have $k_{3b} \ll k_{3f}$. Similarly, for the second elementary step where the equilibrium coefficient $\gamma_2 \approx 1$ the conversion of EP to ES is kinetically more favorable than the conversion in the opposite direction, i.e. $k_{2f} \ll k_{2b}$. These cases are illustrated in the right-hand part of the energy diagram (Fig. 5). We can see that the free activation energies of dissociation of the complex EP , which are inversely proportional to the kinetic rate constants k_{2b} and k_{3f} , are small. In turn, this leads to infinitesimal levels of concentration of the enzyme-product complex. In contrast to the intermediate and the last elementary step where the ratio between kinetic rate constants are well defined, the ratio of the kinetic constants in the first step can vary leading to several alternative energy profiles for ES as shown in Fig. 5. Depending on the concentration levels of E and ES the first elementary step can be kinetically more favorable in the forward or in the backward direction, or to be in the kinetic equilibrium. This scenario corresponds to the structure of irreversible Michaelis-Menten, well-known in the literature (Heinrich and Schuster, 1996), where an enzyme appears predominantly in the reversibly interconvertible forms of the free enzyme E and the enzyme-substrate complex ES , and the product P is irreversibly produced from the enzyme-substrate complex.*

• *The last elementary step has large displacement from its equilibrium ($\gamma_3 \ll 1$), $\gamma_1 = \gamma_2 \approx 1$, and the ES intermediate complex appears with a low probability.* Under these conditions we have $k_{1f} \ll k_{1b}$ and $k_{2f} \gg k_{2b}$, which implies that the enzyme-substrate complex, ES, dissociates rapidly and that its concentration levels are very low. The corresponding energy diagrams are represented in the panel A of Fig. 6. In the last elementary step, there are several alternative activation energy profiles depending on the relative concentration of the free enzyme with respect to the enzyme-product complex, EP.

• *The intermediary step has large displacement from the equilibrium ($\gamma_2 \ll 1$), γ_1 and γ_3 are close to 1, and the probability of the formation of EP is low.* The Gibbs energy profiles depicting this type of reactions are given in the panel B of Fig. 6. These energy profiles are similar to the ones shown in Fig. 5 with a difference in the ratios between k_{3b} and k_{3f} , and k_{2b} and k_{2f} which are slightly less pronounced. Consequently, the free activation energies of the dissociation of EP are slightly increased.

We have generated populations of the enzyme species and computed the elasticities according to the conditions of three scenarios (Table 3). In all three cases, the distributions of the elasticities match the irreversible Michaelis-Menten kinetics (Fig. 4, panel B: distribution for scenario (i); distributions for scenarios (ii) and (iii) are similar and not shown). We observe, as expected, that the flux elasticities with respect to the substrate are uniformly distributed between 0 and 1, and that the ones with respect to the product are close to zero.

Using partial information

We have shown that when no *a priori* information about a reaction is available it is possible to generate populations of corresponding elasticities by sampling efficiently a simplex in the space of enzyme states. Any additional experimental information about the reaction will help in reducing the sampling

space which in turn will allow more accurate computational predictions of the responses of the enzymes to changes in metabolites concentrations and parameters. This exchange of information between computational and experimental studies will result in both better computational models and better design of experiments. Toward this end, we developed a framework to incorporate the additional experimental data in the procedure of computing the elasticities.

As an illustration, we consider again the reaction consisting of three enzymatic elementary steps (Fig. 1). We assume that experimentally observed data suggest that the enzyme appears in its free form E with the probability of 60%, and in the form of enzyme-metabolites complexes ES and EP with the probabilities of 15% and 25%, respectively. We approximate the observed distribution of the experimental data with the Dirichlet distribution whose parameters can be estimated based on the mean values and variances of the acquired data. When estimating the parameters of Dirichlet distribution we consider the fact that the bigger the sum of the parameters is, the smaller the variance becomes. Consequently, by multiplying the vector of parameters with a positive constant bigger than 1, one can reduce the variance of the distribution. More details of this procedure are given in Methods and references therein. The probability density function f_D that approximates the experimental distribution is shown in Fig. 7, panel A, and the corresponding 2000 generated samples are shown in panel B. It is observed that the prescribed marginal distributions for E , ES and EP are well approximated. In Fig. 7, panel B, we also show 2000 data points generated through uniform sampling of simplex which can be used in the case when experimental information is not available. As expected, the density of sampling when partial information is included is higher which allows more thorough characterization of the kinetic space.

Computational efficiency and scalability

In this work, we express the elasticities as a function of a fractional distribution of the enzyme among its states and the displacement from the thermodynamic equilibrium of the enzymatic steps. This mathematical formulation abolishes the need for the knowledge of the ranges of allowable values for the parameters of reactions and allows for efficient generation of populations of elasticities within biochemical networks. We have illustrated that in the process of generation of all plausible elasticities for the three-step kinetic mechanism, instead of sampling from the whole three-dimensional space of enzyme states E/E_T , ES/E_T and EP/E_T , it is sufficient to sample from the surface of the simplex defined in Eq. 3. In other words, the sampling space is significantly reduced. Moreover, each sample generated by the generator of random numbers is directly mapped to this surface so that the computational efforts are marginally increased compared to these of a random generator (see Algorithms 1 and 2). For more complex kinetic mechanisms involving several metabolites, the reduction of the sampling space is even more pronounced, and the computational costs of sampling from simplices are comparable to the ones of generating populations of random vectors. For example, the computational costs of generating the elasticities for a rapid equilibrium random Bi Bi kinematic mechanism which has seven-dimensional enzyme states space approximately equals the costs of generating populations of random vectors with 7 elements.

In the case of large biochemical networks, the elasticities, which are needed for the computation of control coefficients, are generated for each individual reaction. So, computational costs of generation of elasticities scale linearly with the number of reactions in the model. However, when the samples of elasticities are recombined to compute the network control coefficients, additional statistical analyses are needed to ensure that the ergodicity hypothesis is verified papoulis1991. Considering the efficiency of the generation of elasticities, modern computers largely provide the required computational resources.

Conclusions

In spite of advances in measurement techniques, development of kinetic models is a challenging task because kinetic data are still of limited availability and come with the inevitable uncertainty. The variability and incompleteness of data call upon optimization and risk analysis methods such as ORACLE (Mišković and Hatzimanikatis, 2010) that are able to quantify the uncertainty and to integrate available experimental data into models providing reliable predictions/expectations of the behavior of biochemical pathways in the face of perturbations. The formalism presented here allows us to generate and study all biochemically and thermodynamically plausible kinetic models of biochemical reactions thus paving the way for the development of the framework for uncertainty modeling of the kinetics in biochemical pathways. Specific mathematical formulation of the underlying problem allows for efficient generation of populations of kinetic models and enables to scale this methodology even to genome-scale biochemical pathways.

The computed elasticities along with the concentrations of the metabolites allow for the computation of distributions of eigenvalues of the steady states of the biochemical networks thus providing the foundation for the extension of the method for the study of dynamical properties of biochemical networks.

Methods

Systems-oriented models of enzyme kinetics

Assuming a spatial homogeneity in a biochemical reaction, the dynamic behavior of the concentrations of enzyme states, such as E , ES and EP , can be described by a set of ordinary differential equations of the following form:

$$\frac{dx_e}{dt} = Mu(x_e, p), \quad (9)$$

where x_e represents the m -dimensional vector of the concentrations of enzyme species, M denotes the $m \times n$ -dimensional matrix describing the stoichiometry of the reaction, u is the n -dimensional vector of metabolic fluxes within this reaction, referred in the sequel as the internal metabolic fluxes, and p is the vector of parameters defined in Eq. 2. In this mathematical representation, a reversible flux is expressed as a difference between the corresponding forward irreversible and backward irreversible fluxes (Wang et al., 2004).

The conservation relation between enzyme states introduces a rank deficiency of the stoichiometric matrix M . To overcome this, the vector of concentrations x_e can be decomposed in two sub-vectors: an independent enzyme states concentration vector x_{ei} , and a dependent enzyme states concentration vector x_{ed} (Reder, 1988).

In addition, the rows in the stoichiometric matrix M corresponding to the mass balances of the dependent enzyme states can be eliminated so that a new, reduced, stoichiometric matrix M_R is formed (Heinrich and Schuster, 1996; Reder, 1988). Therefore, the mass balance equations of the metabolic reaction (Eq. 9) are reduced to the following form

$$\frac{dx_{ei}}{dt} = M_R u(x_{ei}, x_{ed}(x_{ei}, p), p). \quad (10)$$

Elasticities

We apply the log(linear) kinetic formalism of MCA for the calculation of elasticities in a (bio)chemical reaction (Hatzimanikatis et al., 1996; Hatzimanikatis and Bailey, 1996, 1997). Metabolite elasticities $\varepsilon_p^{x_e}$, and flux elasticities ε_p^u quantify the variations of enzyme states concentrations and internal metabolic fluxes, respectively, with respect to the variations in system parameters. As discussed earlier, if one considers the single enzyme as the system, with the concentrations of the metabolites, S and P , being the parameters, these quantities are in fact the control coefficients. From the same perspective, the enzyme states can be considered as metabolites. Nevertheless, we consider the enzymes as a part

of metabolic networks, hence we refer $\varepsilon_p^{x_e}$ and ε_p^u as the elasticities. The expressions for these elasticities can be derived by linearizing and scaling the system (Eq. 10) around the steady-state:

$$\varepsilon_p^{x_{ei}} = -(M_R U \Xi)^{-1} M_R U \Pi \quad (11)$$

$$\varepsilon_p^u = \Xi \varepsilon_p^{x_{ei}} + \Pi \quad (12)$$

where U denotes the diagonal matrix of the internal steady-state fluxes, and $\Xi = \Xi_i + \Xi_d Q_i^d$ is the matrix of the local sensitivities with respect to the enzyme state concentrations; Ξ_i and Ξ_d are the matrices of the elasticities with respect to independent and dependent enzyme states, respectively, and Q_i^d represents the relative abundance of the dependent enzyme states compared to that of the independent ones. The matrix $\Pi = [\Pi_t, \Pi_r, \Pi_n]$ denotes the local sensitivities with respect to the system parameters, $p^T = [p_t^T, p_r^T, p_n^T]$. The matrix Π_t can be expressed as $\Pi_t = \Xi_d Q_t$ where the weight matrix Q_t represents the relative abundance of dependent enzyme states with respect to the amounts of their corresponding total enzymes.

Equilibrium factors

We define the equilibrium coefficient as the ratio of the backward and the forward reaction rates u_b and u_f , respectively:

$$\gamma = \frac{u_b}{u_f} = \frac{u_f - u_{net}}{u_f} \quad (13)$$

with u_{net} denoting the net flux rate. The equilibrium coefficient, $\gamma \in [0, +\infty)$, reflects the reversibility of a reaction with respect to the net flux. Values of γ close to zero, $\gamma \rightarrow 0$, or close to infinity, $\gamma \rightarrow \infty$, indicate forward irreversible and backward irreversible reaction steps, respectively. In contrast, the values of γ close to 1, $\gamma \approx 1$, imply that the net flux is negligible with respect to backward and forward fluxes, i.e. the enzyme operates near thermodynamic equilibrium.

For a reaction with one product and one substrate, the displacement from the thermodynamic equilibrium can be defined as follows :

$$\Gamma = \frac{S_{eq} P}{P_{eq} S} = \frac{1}{k_{eq}} \frac{P}{S} \quad (14)$$

with S_{eq} and P_{eq} being respectively the concentration of the substrate and the product at the thermodynamic equilibrium (Heinrich and Schuster, 1996). k_{eq} denotes the equilibrium constant defined as a ratio between the products of the forward and the backward rate constants, respectively. Without any loss of generality, we assume that there is a net production of the product P , i.e. $\Gamma < 1$ or $S_{eq} P / P_{eq} S < k_{eq}$, which implies that the Gibbs free energy difference is negative, i.e. $\Delta G < 0$. The displacement from the thermodynamic equilibrium Γ can readily be extracted from the experimentally observed data.

Monte Carlo Sampling Over the Constrained Kinetic Space

We have shown that by sampling the enzyme states while preserving the conservation of the amount of the total enzyme, the uncertainty in the elasticities can be modeled and analyzed statistically in order to characterize the rate-limiting steps. We further extend the proposed idea to address the more general case, to a more complex group of kinetic mechanisms where the enzyme in its free form and enzyme complexes appear linearly in the rate equations. For this kind of kinetic mechanisms, the matrices Ξ and Π , as in the case of the irreversible Michaelis-Menten kinetics, can be expressed as functions of ratios of the enzymes states and the amount of the total enzyme E_T . Hence, following the reasoning from the previous section, we can establish a general Monte Carlo methodology allowing us to quantify the elasticities. We assume that details about the kinetic mechanism are available, or, an appropriate kinetics is assumed. The procedure is as follows:

1. Construct the stoichiometry matrix using available biochemical and

genomics information, and separate the enzyme states into an independent and a dependent group.

2. Estimate steady-state fluxes using FBA methods.

3. Generate the random enzyme states samples satisfying the conservation constraints on the amount of total enzyme. If no a priori information about the distribution of the enzyme states is available, the random samples are uniformly generated. Information from acquired experimental data can be included to introduce either a bias in the uniform distribution or even to define other types of distribution.

4. Determine the equilibrium coefficients on the basis of the nature of kinetic mechanism and the knowledge of the equilibrium displacement Γ . If only Γ is known, the bounds on the equilibrium coefficients are precisely defined, thus the space of the equilibrium coefficients can be sampled to generate the populations of the thermodynamically feasible realizations of the underlying reaction.

5. Construct the sensitivity matrices Ξ_i , Ξ_d and Π followed by the computation of the metabolite and flux elasticities according to Eqs. 11 and 12.

In the sequel, we give more details about the generation of the random enzyme states samples mentioned in the third step of the procedure.

Uniform sampling of enzyme states

There exists an abundant literature on random variate generation over different regions (Feller, 1968; Rubinstein, 1981; Devroye, 1986; Garvey, 2000; Gentle, 2003). The most common methods used for uniform sampling are acceptance-rejection methods (Von Neumann, 1963), and Monte Carlo Markov Chain methods (Gilks et al., 1998; Brémaud, 1999). However, the former methods tend to be very inefficient in high dimension space, while the latter require a large number of samples to obtain asymptotically uniform coverage of the space.

In this paper we make use of ideas presented in (Wilks, 1962; Rubinstein, 1982) that exploit the particular structure of the enzyme space we want to sample

uniformly. For a general kinetic mechanism, where an enzyme appears in the free form E and in the form of $n-1$ different enzyme-metabolite complexes $EX_i, i=1, \dots, n-1$, we can write

$$E + \sum_{i=1}^{n-1} EX_i = E_T \Rightarrow \frac{E}{E_T} + \sum_{i=1}^{n-1} \frac{EX_i}{E_T} = 1. \quad (15)$$

In the n -dimensional space of ratios $(.8mm E / -.8mm E_T, .8mm EX_1 / -.8mm E_T, .8mm EX_2 / -.8mm E_T, \dots, .8mm EX_{n-1} / -.8mm E_T)$, the constraint given in Eq. 15 represents a simplex. Observe also that E/E_T and $EX_i/E_T, i=1, \dots, n-1$ are constrained between 0 and 1. An example of a simplex in the three-dimensional space is shown in Fig. 2.

We next use the fact that a random vector uniformly distributed over n -dimensional simplex can be obtained by generating samples from a n -variate Dirichlet distribution with all parameters equal to 1, which will be referred subsequently as $D(1, \dots, 1)$. Generation of random variables from $D(1, \dots, 1)$ can then be performed as follows (Rubinstein, 1982).

Algorithm 1 (*Generating uniform enzyme states*)

1. Generate a random vector (X_1, \dots, X_n) exponentially distributed with the rate parameter equal to 1.
2. Compute the random vector

$$(Y_1, \dots, Y_n) = \left(\frac{X_1}{\sum_{i=1}^n X_i}, \dots, \frac{X_n}{\sum_{i=1}^n X_i} \right). \quad (16)$$

The random vector (Y_1, \dots, Y_n) is distributed with $D(1, \dots, 1)$, i.e. it is uniformly distributed on the surface of n -dimensional simplex. So, Algorithm 1 provides a very efficient and simple way to generate sets of enzyme states

(.8mm E / -.8mm E_T , .8mm EX_1 / -.8mm E_T , .8mm EX_2 / -.8mm E_T , ..., .8mm EX_{n-1} / -.8mm E_T) even in the case of high-dimensional spaces.

Non-uniform sampling of enzyme states

Detailed knowledge of ranges of probability with which an enzyme appears in each of its states can be used to generate more refined sets of enzyme states. Once again, we benefit from the fact that Dirichlet distribution samples naturally from simplex. In contrast to the case of uniform sampling where all parameters of Dirichlet distribution were equal to 1, in this case we change these parameters so that the shape of Dirichlet distribution approximatively corresponds to the experimentally observed data.

The probability density function of the Dirichlet distribution with parameters $\nu_1, \nu_2, \dots, \nu_{n-1}, \nu_n$ is given as

$$f_D(\nu_1, \dots, \nu_n) = \frac{\Gamma\left(\sum_{i=1}^n \nu_i\right)}{\prod_{i=1}^n \Gamma(\nu_i)} \prod_{i=1}^{n-1} \sigma_i^{\nu_i-1} \left(1 - \sum_{i=1}^{n-1} \sigma_i\right)^{\nu_n-1}$$

where $\Gamma(\cdot)$ denotes the gamma function, the random variables $\sigma_1, \dots, \sigma_{n-1} > 0$ satisfy $\sigma_1 + \dots + \sigma_{n-1} < 1$, and the parameters $\nu_1, \dots, \nu_n > 0$. Outside the simplex the probability density function is zero. The Dirichlet distribution has a nice property that can be used in approximating the experimental data. For a random vector (Y_1, \dots, Y_n) distributed with $D(\nu_1, \dots, \nu_n)$ we have that the mean values of each component of the random vector are given as

$$E\{Y_i\} = \frac{\nu_i}{\sum_{k=1}^n \nu_k} \quad (17)$$

and the corresponding variances read as

$$\text{Var}\{Y_i\} = \frac{v_i \left(\sum_{k=1, k \neq i}^n v_k \right)}{\left(1 + \sum_{k=1}^n v_k \right) \left(\sum_{k=1}^n v_k \right)^2}. \quad (18)$$

In addition, the marginal distributions of X_i 's are Beta distributions, i.e. $Y_i \sim \text{Beta}(v_i, v_0 - v_i)$. Hence, we can use information extracted from the experimental data, such as the ranges of the probability in which each of enzyme states appear, to define a mean value and a variance for each of the marginal distributions of enzyme states. So defined mean values and variances are subsequently used to compute the parameters of Dirichlet distribution. In other words, we design the Dirichlet distribution through shaping its marginal distributions. In the case of high-dimensional enzyme states space, the problem of finding the parameters v_1, \dots, v_n can be cast as an optimization problem.

Once having determined the parameters of the Dirichlet distribution that approximates well the experimental data, we turn to the problem of generating the samples of that distribution. In (Arnason, 1972), an efficient method for generating the Dirichlet variates with given parameters $v_1, v_2, \dots, v_{n-1}, v_n$ is proposed. This method is described by the following algorithm.

Algorithm 2 (*Generating non-uniformly sampled enzyme states*)

1. Generate a random vector (X_1, \dots, X_n) distributed with the gamma distributions $G(v_i), i = 1, \dots, n$.
2. Compute the Dirichlet variates as follows:

$$(Y_1, \dots, Y_n) = \left(\frac{X_1}{\sum_{i=1}^n X_i}, \dots, \frac{X_n}{\sum_{i=1}^n X_i} \right). \quad (19)$$

The Dirichlet variates (Y_1, \dots, Y_n) have the probability density function $D(v_1, \dots, v_n)$. Algorithm 2 is a general version of Algorithm 1 and can be used to generate uniform variates as well.

Acknowledgments

The authors would like to thank Ivano Tavernelli and Keng Cher Soh. LM was supported by the NEMO for bioethanol project funded by the European Seventh Framework Programme for research and technological development (FP7). VH was supported by funding from Ecole Polytechnique Fédérale de Lausanne (EPFL), SystemsX.ch and DuPont.

Tables

Table 1: **Definitions.**

Name	Symbol	Definition
Metabolite elasticities	$\varepsilon_p^{x_{ei}}$	$\frac{d \ln x_{ei}}{d \ln p}$
Flux elasticities	ε_p^u	$\frac{d \ln u}{d \ln p}$
Independent enzyme states elasticities	Ξ_i	$\frac{\partial \ln u}{\partial \ln x_{ei}}$
Dependent enzyme states elasticities	Ξ_d	$\frac{\partial \ln u}{\partial \ln x_{ed}}$
Total enzyme parameter elasticities	Π_t	$\frac{\partial \ln u}{\partial \ln p_t}$
Reaction rates elasticities	Π_r	$\frac{\partial \ln u}{\partial \ln p_r}$
Other parameters elasticities	Π_n	$\frac{\partial \ln u}{\partial \ln p_n}$
Relative abundance	Q_i^d	$\frac{\partial \ln x_{ei}}{\partial \ln x_{ed}}$
Total enzyme weights	Q_t	$\frac{\partial \ln x_{ed}}{\partial \ln p_t}$

Table 2: **Elasticities' constitutive elements for the fundamental three-step reversible kinetic mechanism (Fig. 1).** In the expression for the steady-state flux matrix U , U_{net} denotes the steady-state net flux, while $\gamma_i, i=1,2,3$ are the equilibrium coefficients that represent the ratio between the backward reaction rates, u_{ib} , and the forward ones, u_{if} , in each of the elementary reaction steps (see Methods): $\gamma_1 = u_{1b}/u_{1f}$, $\gamma_2 = u_{2b}/u_{2f}$ and $\gamma_3 = u_{3b}/u_{3f}$.

$M_R = \begin{pmatrix} 1 & -1 & -1 & 1 & 0 & 0 \\ 0 & 0 & 1 & -1 & -1 & 1 \end{pmatrix}$	$\Xi = \begin{pmatrix} -ES/E & 1 & 1 & 0 & 0 & -ES/E \\ -EP/E & 0 & 0 & 1 & 1 & -EP/E \end{pmatrix}^T$
$U = \begin{pmatrix} \frac{1}{1-\gamma_1} & 0 & 0 & 0 & 0 & 0 \\ 0 & \frac{\gamma_1}{1-\gamma_1} & 0 & 0 & 0 & 0 \\ 0 & 0 & \frac{1}{1-\gamma_2} & 0 & 0 & 0 \\ 0 & 0 & 0 & \frac{\gamma_2}{1-\gamma_2} & 0 & 0 \\ 0 & 0 & 0 & 0 & \frac{1}{1-\gamma_3} & 0 \\ 0 & 0 & 0 & 0 & 0 & \frac{\gamma_3}{1-\gamma_3} \end{pmatrix} U_{net}$	$\Pi = \begin{pmatrix} E_T/E & & & & & 1 & 0 \\ 0 & & & & & 0 & 0 \\ 0 & & & & & 0 & 0 \\ 0 & & I_{6 \times 6} & & & 0 & 0 \\ 0 & & & & & 0 & 0 \\ E_T/E & & & & & 0 & 1 \end{pmatrix}$

Table 3: **Conditions under which the three-step kinetic mechanism reduces to the irreversible Michaelis-Menten kinetics.**

Scenario	γ_1	γ_2	γ_3	E	ES	EP
(i)	≈ 1	≈ 1	$\ll 1$	uniformly distributed	uniformly distributed	≈ 0
(ii)	≈ 1	≈ 1	$\ll 1$	uniformly distributed	≈ 0	uniformly distributed
(iii)	≈ 1	$\ll 1$	≈ 1	uniformly distributed	uniformly distributed	≈ 0

Figure Captions

Figure 1: **Reversible Michaelis-Menten kinetics consisting of three enzymatic reaction steps.**

Figure 2: **Example of a three-dimensional enzyme states space.** The enzyme appears in the free form E , as the enzyme-substrate complex ES and as the enzyme-product complex EP . The enzyme species are randomly generated over the simplex.

Figure 3: **The surface $\Gamma = \gamma_1\gamma_2\gamma_3$ in the space of elementary displacements γ_1 , γ_2 and γ_3 .** As one approaches to the thermodynamic equilibrium the surface of Γ shrinks, and as a consequence the allowable ranges of γ_1 , γ_2 and γ_3 shrink as well.

Figure 4: **Histograms of the flux elasticities for the three-step reaction away from the equilibrium ($\Gamma = 0.01$).** *Panel A:* the flux elasticities with respect to the substrate S (*upper part*) and the product P (*lower part*) concentrations; the equilibrium coefficients are $\gamma_1 = 0.0104$, $\gamma_2 = 0.98$, and $\gamma_3 = 0.98$; *Panel B:* histograms of elasticities for the irreversible Michaelis-Menten kinetics - the equilibrium coefficients are $\gamma_1 = \gamma_2 = 0.98$, and $\gamma_3 = 0.0104$.

Figure 5: **Gibbs free energy profiles for the reaction following the irreversible Michaelis-Menten kinetics.** The last elementary step is largely displaced from the equilibrium ($\gamma_3 \ll 1$), while the other two steps are close to the equilibrium. High values of the rate constants k_{3f} and k_{2b} result in a very low

concentration levels of EP . The Gibbs energy levels of substrate, intermediates and product are given in dark blue, whereas the transition states are traced in red. For different pairs of concentration levels for E and ES several alternative energy configurations can be distinguished as shown with light gray curves. The corresponding energy levels are traced in light blue.

Figure 6: **Reaction energy profiles for the reactions characterized in scenarios (ii) and (iii).** *Panel A:* High values for k_{1b} and k_{2f} constants drive the concentration levels of ES very low. The equilibrium displacements $\gamma_3 \ll 1$, $\gamma_1 = \gamma_2 \approx 1$. *Panel B:* The equilibrium displacement predominantly expressed in the intermediary reaction step. The concentration levels of EP substantially smaller than the ones of E and ES . The alternative energy levels for ES shown in light blue.

Figure 7: **Non-uniform sampling of enzyme space.** *Panel A:* probability density function f_D as a function of the simplex $\frac{E}{E_T} + \frac{ES}{E_T} + \frac{EP}{E_T} = 1$ lying in the horizontal plane. This distribution allows for generating random sets of enzyme states for a reaction where the enzyme is in its forms E , ES and EP with probability of 60%, 15% and 25%, respectively; *Panel B:* uniform sampling (dots) and biased sampling (diamonds) with the probability density function f_D presented in Panel A. Samples presented in the space $(E/E_T, ES/E_T, EP/E_T)$.

References

E. Almaas, B. Kovacs, T. Vicsek, Z. N. Oltvai, and A. L. Barabasi. Global organization of metabolic fluxes in the bacterium *escherichia coli*. *Nature*, 427: 839--843, 2004.

R. Alves and M. A. Savageau. Systemic properties of ensembles of metabolic networks: application of graphical and statistical methods to simple unbranched pathways. *Bioinformatics*, 16: 534--547, 2000.

A. N. Arnason. Simple, exact, efficient methods for generating Beta and Dirichlet variates. *Utilitas Matematica*, 1: 249--290, 1972.

D. A. Beard and H. Qian. *Chemical Biophysics - Quantitative Analysis of Cellular Systems*. Cambridge texts in biomedical engineering. Cambridge University Press, Cambridge, UK, 2008. ISBN 978-0521870702.

R. Breitling, D. Vitkup, and M. Barrett. New surveyor tools for charting microbial metabolic maps. *Nature Reviews Microbiology*, 6: 156--161, 2008.

P. Brémaud. *Markov Chains*. Springer, Berlin, 1999. ISBN 0387985093.

C. Contador, M. Rizk, J. Asenjo, and J. Liao. Ensemble modeling for strain development of l-lysine-producing *escherichia coli*. *Metabolic Engineering*, 11: 221--233, Jan 2009.

A. Cornish-Bowden and M. L. Cardenas. *Technological and Medical Implications of Metabolic Control Analysis*. NATO science series. Kluwer Academic Publishers, Dordrecht, The Netherlands, 2000. ISBN 978-0792361893.

L. Devroye. *Non-Uniform Random Variate Generation*. Springer-Verlag, Berlin, 1986.

W. Feller. *An Introduction to Probability Theory and Its Applications, Volume 1*. Wiley, New York, January 1968.

P. Garvey. *Probability Methods for Cost Uncertainty Analysis*. Marcel Dekker, Inc., New York, 2000.

J. Gentle. *Random Number Generation and Monte Carlo Methods*. Springer,

Berlin, 2003. ISBN 0387001786.

W. Gilks, S. Richardson, and D Spiegelhalter, editors. *Markov Chain Monte Carlo in Practice*. Chapman & Hall, London, 1998. ISBN 0412055511.

R. Goodacre, S. Vaidyanathan, W. B. Dunn, G. G. Harrigan, and D. B. Kell. Metabolomics by numbers: acquiring and understanding global metabolite data. *Trends Biotechnology*, 22: 245--252, 2004.

S. Grimbs, J. Selbig, S. Bulik, H. Holzhuetter, and R. Steuer. The stability and robustness of metabolic states: identifying stabilizing sites in metabolic networks. *Molecular Systems Biology*, 3, Nov 2007.

V. Hatzimanikatis and J. E. Bailey. MCA has more to say. *Journal of Theoretical Biology*, 182 (3): 233--242, Oct 7 1996. ISSN 0022-5193.

V. Hatzimanikatis and J. E. Bailey. Effects of spatiotemporal variations on metabolic control: Approximate analysis using (log)linear kinetic models. *Biotechnology and Bioengineering*, 54 (2): 91--104, APR 20 1997. ISSN 0006-3592.

V. Hatzimanikatis, C. A. Floudas, and J. E. Bailey. Analysis and design of metabolic reaction networks via mixed-integer linear optimization. *AIChE Journal*, 42 (5): 1277--1292, May 1996. ISSN 0001-1541.

R. Heinrich and S. Schuster. *The Regulation of Cellular Systems*. Chapman & Hall, New York, 1996.

N. Jamshidi and B. Palsson. Formulating genome-scale kinetic models in the post-genome era. *Molecular Systems Biology*, 4 (171), Jan 2008.

N. Jamshidi and B. Palsson. Mass action stoichiometric simulation models: Incorporating kinetics and regulation into stoichiometric models. *Biophysical Journal*, 98: 175--185, 2010.

B. Kholodenko, H. Westerhoff, and G. Brown. Rate limitation within a single enzyme is directly related to enzyme intermediate levels. *FEBS Letters*, 349: 131--134, Jan 1994.

W. Liebermeister and E. Klipp. Bringing metabolic networks to life: convenience rate law and thermodynamic constraints. *Journal of Theoretical Biology*, 3 (41), 2006.

L. Mišković and V. Hatzimanikatis. Production of biofuels and biochemicals: in need of an ORACLE. *Trends in Biotechnology*, 28 (8): 391--398, 2010.

D. L. Nelson and M. M. Cox. *Lehninger Principles of Biochemistry*. W.H. Freeman, San Francisco, USA, 2005. ISBN 9780716743392.

S. B. Petkov and C. Maranas. Quantitative assesment of uncertainty in the optimization of metabolic pathways. *Biotechnology and Bioengineering*, 56: 145--161, 1997.

C. Reder. Metabolic control theory: a structural approach. *J. Theor. Biol.*, Jan 1988.

M. Rizk and J. Liao. Ensemble modeling for aromatic production in escherichia coli. *PLoS One*, 4, September 2009.

J. Ross. *Thermodynamics and Fluctuations far from Equilibrium*. Springer series in chemical physics. Springer, Berlin, Heidelberg, New York, 2008. ISBN 978-3540745549.

R. Rubinstein. *Simulation and the Monte Carlo method*. John Wiley & Sons, New York, 1981.

R. Rubinstein. Generating random vectors uniformly distributed inside and on the surface of different regions. *Europ. J. Oper. Res.*, pages 205--209, Jan 1982.

J. Schellenberger and B. Palsson. Use of randomized sampling for analysis of metabolic networks. *Journal of Biological Chemistry*, 284 (9): 5457--5461, 2009.

R. Steuer, T. Gross, J. Selbig, and B. Blasius. Structural kinetic modeling of metabolic networks. *Proceedings of PNAS*, 103 (32): 11868--11873, 2006.

B. Teusink, J. Passarge, C. A. Reijenga, E. Esgalhadó, C. C. van der

Weijden, M. Schepper, M. C. Walsh, B. M. Bakker, K. van Dam, H. V. Westerhoff, and J. L. Snoep. Can yeast glycolysis be understood in terms of in vitro kinetics of the constituent enzymes? Testing biochemistry. *European Journal of Biochemistry*, 267: 5313--5329, 2000.

S. Thomas and D. A. Fell. Metabolic control analysis - sensitivity of control coefficients to experimentally determined variables. *Theoretical Biology and Medical Modelling*, 167: 175--200, 1994.

L. Tran, M. Rizk, and J. Liao. Ensemble modeling of metabolic networks. *Biophysical Journal*, 95: 5606--5617, December 2008. doi: 10.1529/biophysj.108.135442 .

A. Varma and B. O. Palsson. Metabolic capabilities of escherichia-coli. I synthesis of biosynthetic precursors and cofactors. *Journal of Theoretical Biology*, 165 (4): 477--502, 1993 a .

A. Varma and B. O. Palsson. Metabolic capabilities of escherichia-coli .2. optimal-growth patterns. *Journal of Theoretical Biology*, 165 (4): 503--522, 1993 b .

J. Von Neumann. Various techniques used in connection with random digits. *Collected Works*, pages 768--770, 1963.

L. Wang, I. Birol, and V. Hatzimanikatis. Metabolic control analysis under uncertainty: Framework development and case studies. *Biophysical Journal*, 87: 3750--3763, Jan 2004. URL <http://www.biophysj.org/cgi/content/abstract/87/6/3750> .

L. Q. Wang and V. Hatzimanikatis. Metabolic engineering under uncertainty. i: Framework development. *Metabolic Engineering*, 8 (2): 133--141, 2006 a .

L. Q. Wang and V. Hatzimanikatis. Metabolic engineering under uncertainty - ii: Analysis of yeast metabolism. *Metabolic Engineering*, 8 (2): 142--159, 2006 b .

Accepted Preprint

S. S. Wilks. *Mathematical Statistics*. Wiley, New York, December 1962.

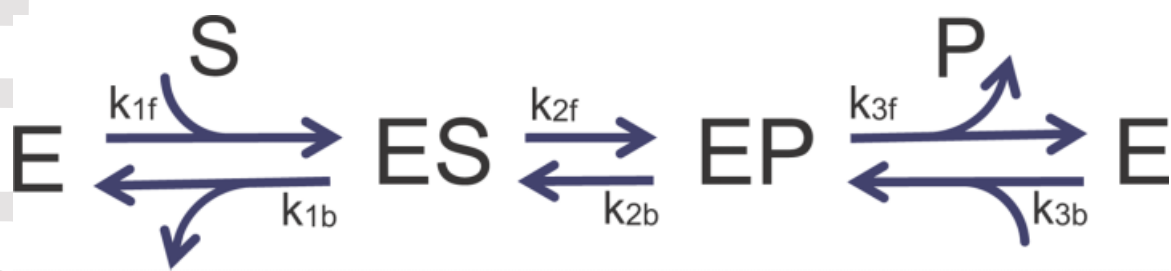


Figure 1.

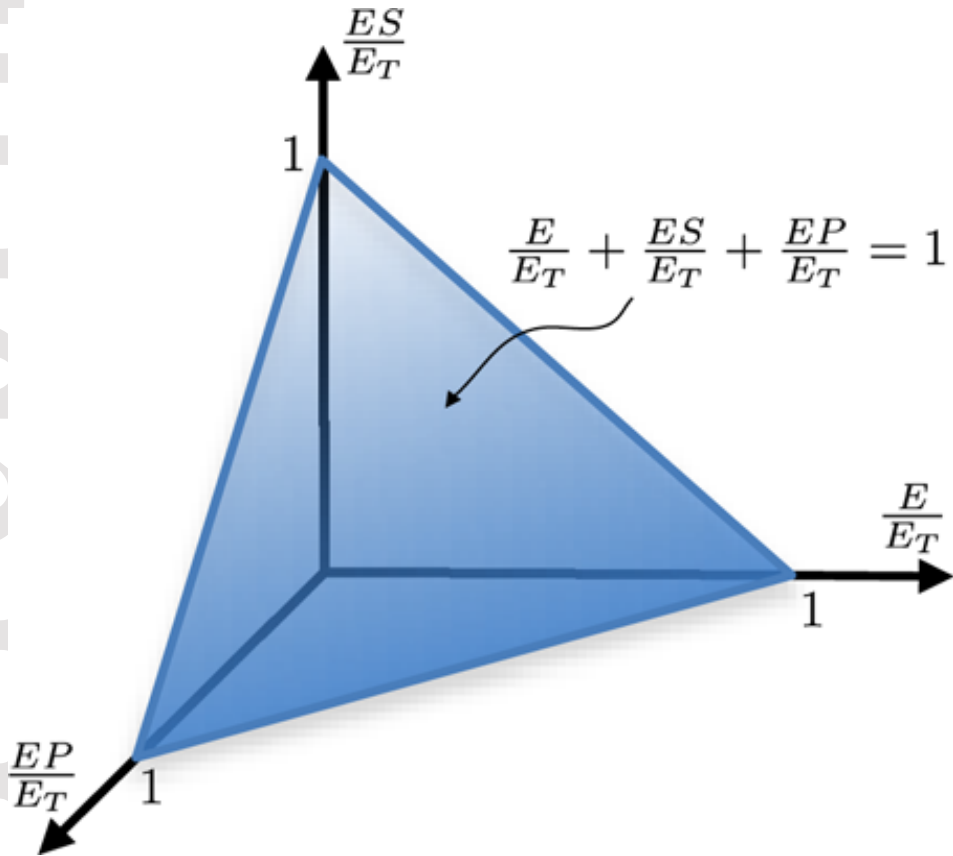


Figure 2.

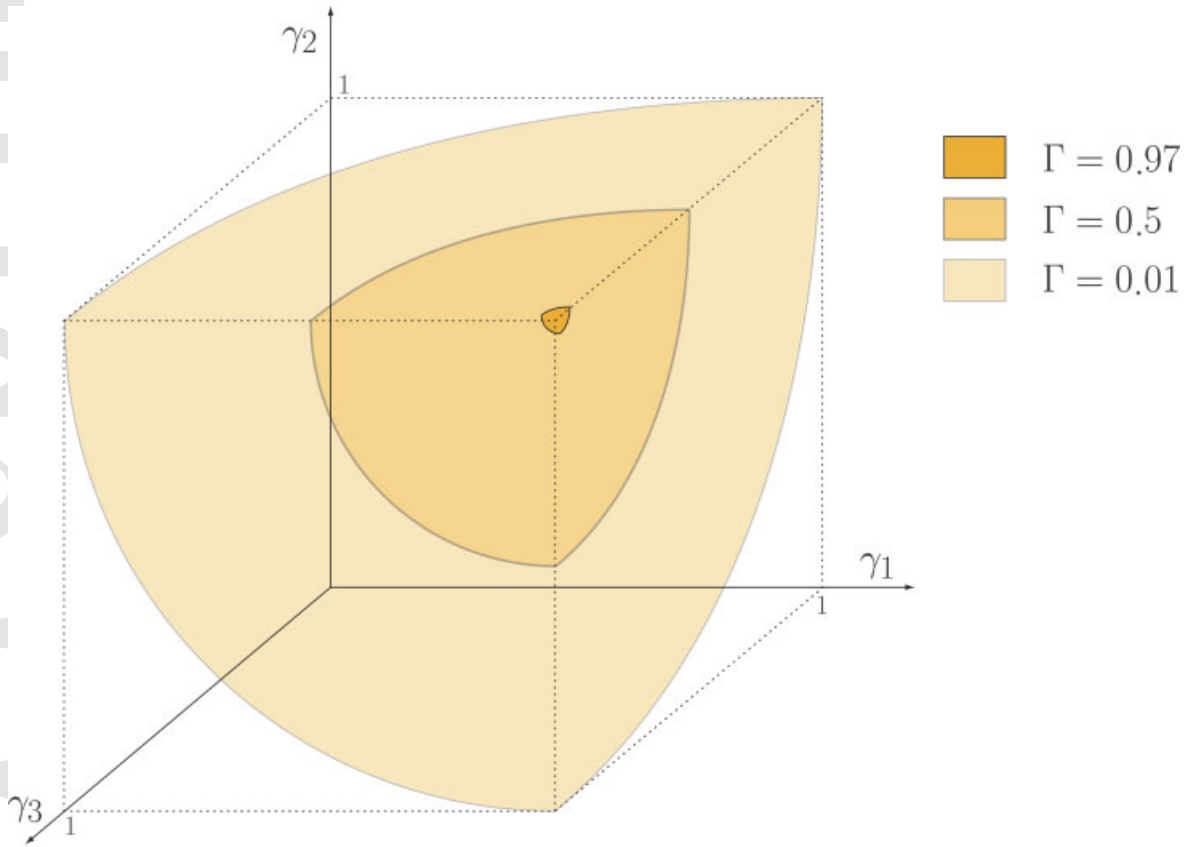


Figure 3.

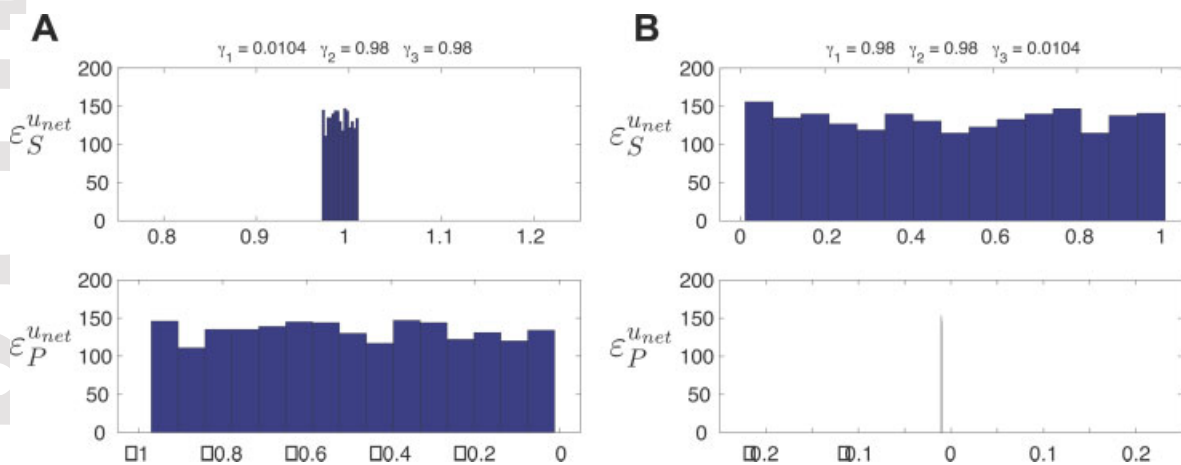


Figure 4.

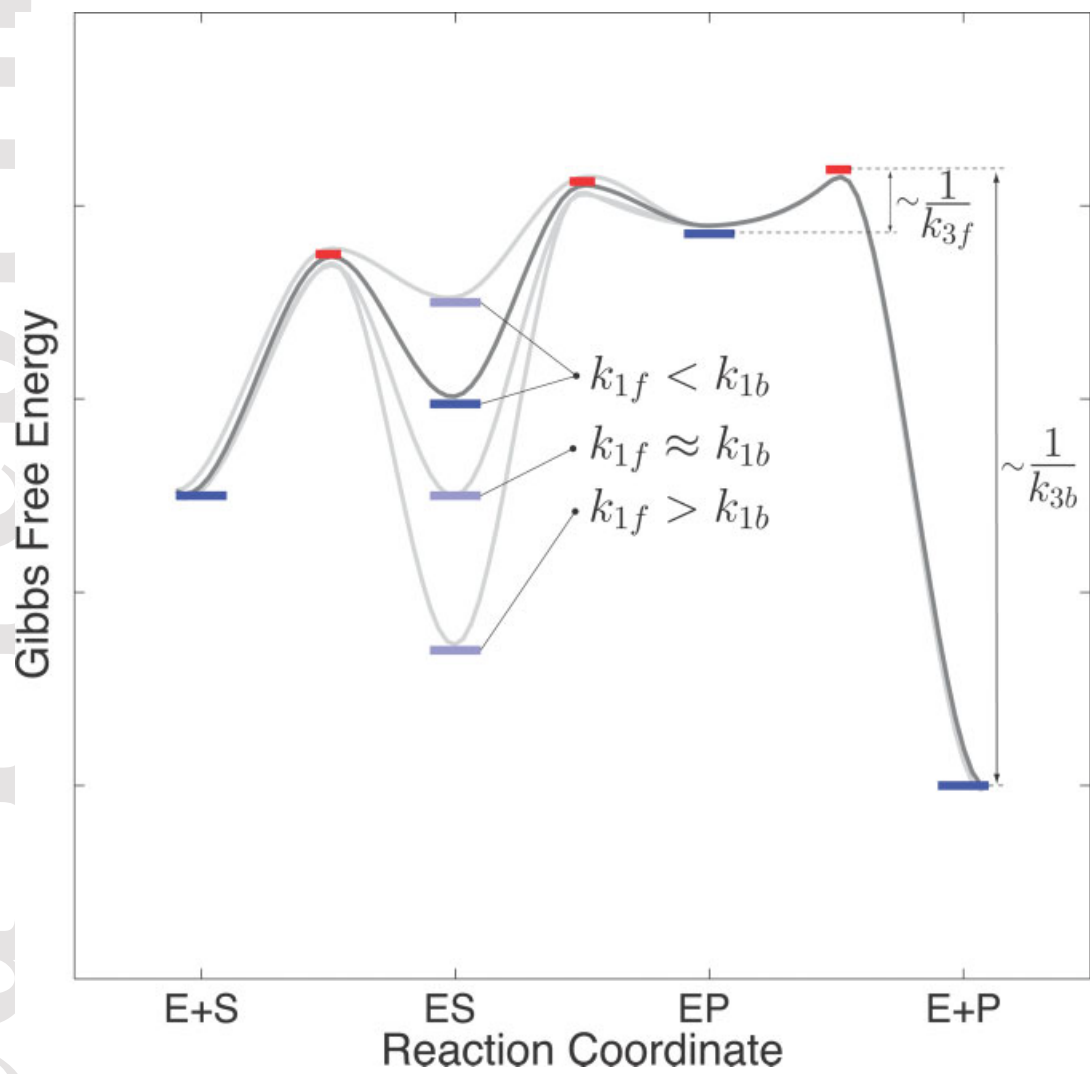


Figure 5.

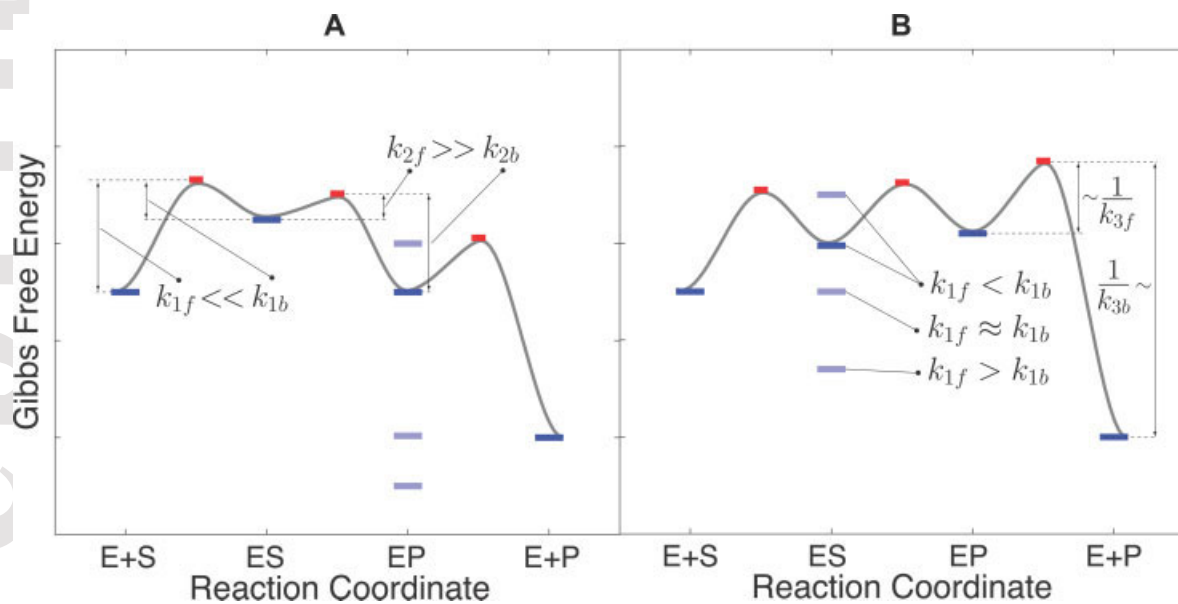


Figure 6.

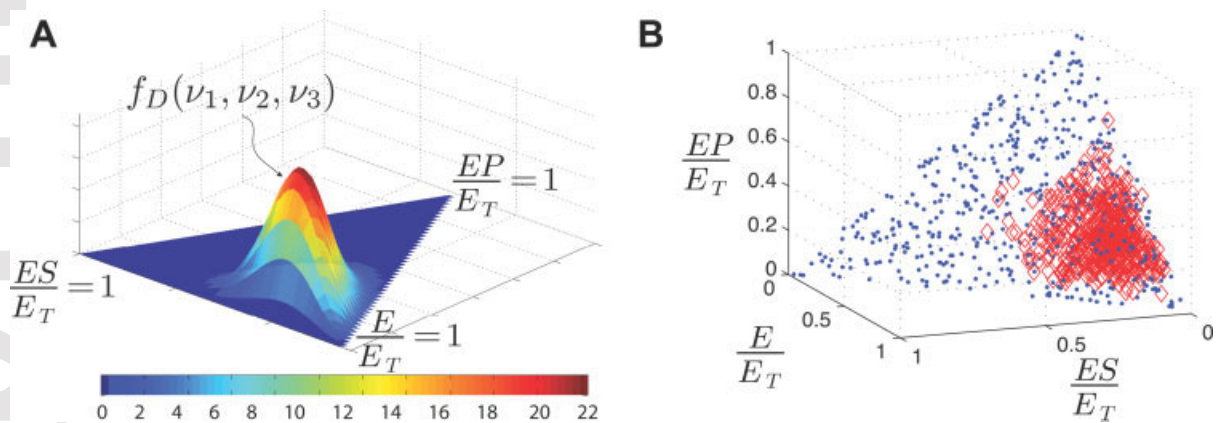


Figure 7.